Supporting Information

Synergistic enhancement of the photoelectrochemical water splitting performance of $BiFeO_3$ photocathodes via potassium doping and surface platinum modification

Sijie Wen,[a,b,c] *Guangping Yi,*[a,b,c] *Yiping Zhao,*[a,b,c] *Xiaofan Yang,*[b,e] *Pengfei Lv,*[a,b,c] *Zhao Jing,*[b,e] *Qiang Wang,*[b,d] *and Pengyi Tang*[a,b,c,]*

[a] National Key Laboratory of Materials for Integrated Circuits, Shanghai Institute of Microsystem and Information Technology, Chinese Academy of Sciences, Shanghai 200050, China

[b] 2020 X-Lab, Shanghai Institute of Microsystem and Information Technology, Chinese Academy of Sciences, Shanghai 200050, China

[c] School of Graduate Study, University of Chinese Academy of Sciences, Beijing 100049, China

[d] State Key Laboratory of Transducer Technology, Shanghai Institute of Microsystem and Information Technology, Chinese Academy of Sciences, Shanghai 200050, China

[e] School of Mechanical and Power Engineering, East China University of Science and Technology, Shanghai 200237, China

* Corresponding author: E-mail: py.tang@mail.sim.ac.cn (Pengyi Tang).

Experimental section

Photocathodes synthesis

Materials

Unless otherwise specified, all commercially available reagents and solvents were used as received without further purification. The reagents used in this work include: Bismuth nitrate pentahydrate ($Bi(NO_3)_3 \cdot 5H_2O$, Aladdin, ≥99%), Iron nitrate nonahydrate ($Fe(NO_3)_3 \cdot 9H_2O$, Sigma-Aldrich, ≥98%), 2-Methoxyethanol (Adamas, ≥99%), Acetic acid (Adamas, ≥99%), Potassium nitrate (Aladdin, 99%), Lithium nitrate (Adamas, ≥99%), Cesium chloride (Adamas, ≥99%), Potassium chloroplatinate (K_2PtCl_4, Adamas, ≥98%), and Anhydrous sodium sulfate (Na_2SO_4, Greagent, ≥99%).

Preparation of K-BFO Photocathodes

K^+ doped $BiFeO_3$ (abbreviated as K-BFO) photocathodes were prepared via a solution spin-coating method, with fluorine-doped tin oxide (FTO) conductive glass used as the substrate. Prior to spin-coating, the FTO conductive glass was sequentially ultrasonically cleaned in acetone, anhydrous ethanol, and deionized water for 10 min each to thoroughly remove surface impurities. Bismuth nitrate pentahydrate (0.97 g) and iron nitrate nonahydrate (0.808 g) were weighed according to a 1:1 molar ratio of Bi to Fe, and potassium nitrate was simultaneously added as the doping source to adjust the molar ratio of doping element K to Fe in the range of 2%~8%, with four experimental gradients set at 2%, 4%, 6% and 8%. The above reagents were co-dissolved in a mixed solvent composed of 4 mL of 2-methoxyethanol and 2 mL of glacial acetic acid, and ultrasonicated for 30 min to obtain a homogeneous and stable doped precursor solution. Using a pipette, 50 μL of the precursor solution was uniformly dropped onto the surface of the FTO substrate, and spin-coating of a single-layer film was completed with a spin coater set at a rotation speed of 3000 rpm and a spin-coating duration of 30 s. After each spin-coating process, the obtained sample

was immediately placed on a heating platform and dried at 60 ℃ for 30 min. The spin-coating-drying cycle was repeated 4 times to complete the film fabrication. After the spin-coating process, the sample was first placed in a muffle furnace for pre-annealing at 300 ℃ for 30 min, and then heated to 600 ℃ and held for 120 min to complete the crystallization process, finally obtaining the K-BFO photocathodes.

Preparation of BFO Photocathodes Doped with Other Elements

BFO Photocathodes doped with Li^+ and Cs^+ were prepared with exactly the same process as the above K-BFO photocathodes, except that the doping sources in the precursor solution were replaced with lithium nitrate and cesium chloride correspondingly. The molar ratios of the doping elements to Fe were also set to four gradients of 2%, 4%, 6% and 8%, while the rest of the precursor preparation, film spin-coating, drying, annealing and crystallization processes remained unchanged. Finally, BFO-based photocathodes with different doping concentrations and different doping elements were fabricated for PEC performance screening and comparison of alkali metal dopants.

Preparation of K-BFO/Pt Photocathodes

K-BFO/Pt photocathodes were prepared via an electrochemical deposition method, where Pt nanoparticle co-catalysts were supported on the surface of K-BFO photocathodes with the optimal doping ratio. In the experiment, 0.1 g of potassium chloroplatinate was added to 100 mL of deionized water and continuously stirred until complete dissolution to obtain an electrolyte for Pt nanoparticle deposition. The deposition experiment was carried out in a standard three-electrode electrochemical system, with a platinum sheet electrode as the counter electrode, an Ag/AgCl electrode as the reference electrode, and the K-BFO thin film photocathode with the optimal doping ratio as the working electrode. In the potentiostatic mode, the deposition potential was set to 0.4 V vs. RHE, and the total deposition charge was controlled at 5 mC to complete the uniform loading of Pt nanoparticles on the electrode surface, finally fabricating the K-BFO/Pt photocathodes.

Structural and morphological characterization

The crystalline structure of photocathodes was characterized by X-ray diffraction (XRD) on a Bruker D8 ADVANCE instrument over a 2θ range of 25-60° at a scanning rate of 5°/min. UV-vis absorption spectra were collected with a SHIMADZU UV-2600i spectrophotometer. X-ray photoelectron spectroscopy (XPS) data were acquired using an ESCALAB 250xi and a Thermo Scientific K-Alpha spectrometer. Scanning electron microscopy (SEM) images were obtained with a ZEISS Sigma 300 microscope. Photoluminescence (PL) spectra were measured at room temperature on an Edinburgh FLS 1000 fluorescence spectrometer under 360 nm laser excitation. Time-resolved photoluminescence (TRPL) decay was recorded at 475 nm using the same Edinburgh FLS 1000 system.

Photoelectrochemical and electrochemical measurements

All photoelectrochemical measurements were conducted at room temperature using an electrochemical workstation (CHI760E and Metrohm Autolab PGSTATM204) equipped with a conventional three-electrode cell. The prepared photocathodes served as the working electrode (WE), a silver/silver chloride (Ag/AgCl) electrode was used as the reference electrode (RE), and a Pt electrode functioned as the counter electrode (CE). The temperature was maintained at 25 °C using a water-cooling system. Illumination was provided by a xenon (Xe) lamp (CEAULIGHT CEL-S500) equipped with an air mass (AM) 1.5G filter, and the light intensity was calibrated to 100 $mW \cdot cm^{-2}$ at the WE. The exposed area of the photocathode was 1 cm^2 (1 cm × 1 cm), and all photoelectrochemical tests employed back-side illumination through the FTO side. A 0.5 M sodium sulfate solution was used as the electrolyte. The potential conversion was calculated using the Nernst equation (1):

$$E_{RHE} = E_{Ag/AgCl} + 0.059 \times pH + 0.1976 \quad (V) \quad (1)$$

The incident photon-to-current efficiency (IPCE) was measured at 0.4 V vs.

RHE in 0.5 M Na_2SO_4 solution, and was calculated using the following equation (2):[1]

$$\mathrm{IPCE} = \left|\frac{1240 \times J}{\lambda \times P_{\lambda}}\right| \times 100\% \#(2)$$

Where J is the photocurrent density ($mA \cdot cm^{-2}$) at a specific wavelength, λ is the wavelength (nm) of the incident light, and P_{λ} is the incident light power density ($mW \cdot cm^{-2}$) at that wavelength.

Mott-Schottky (M-S) plots were measured at an AC frequency of 1000 Hz under dark conditions, with an applied bias ranging from 0.2 to 1.2 V vs. RHE. The carrier density (N_a) and flat-band potential (E_{fb}) of the photocathodes were determined by fitting the linear segment of the M-S curve. The specific calculation formulas are shown in equation (3) and equation (4):

$$\frac{1}{C^2} = \frac{2}{e \varepsilon \varepsilon_0 N_a}\left[\left(E_{fb} - E\right) - \frac{k_B T}{e}\right] \#(3)$$

$$N_a = -\frac{2}{e \varepsilon \varepsilon_0}\left[\frac{\mathrm{d}\left(\frac{1}{C^2}\right)}{\mathrm{d}V}\right]^{-1} \#(4)$$

where C is the space charge layer capacitance ($F \cdot cm^{-2}$) of the photocathode, e is the elementary charge (1.602×10^{-19} C), ε is the relative dielectric constant of $BiFeO_3$, ε_0 is the vacuum permittivity (8.854×10^{-14} $F \cdot cm^{-1}$), N_a is the acceptor carrier concentration (cm^{-3}) of the p-type $BiFeO_3$ photocathode, E is the applied potential (V vs. RHE), E_{fb} is the flat-band potential (V vs. RHE), k_B is the Boltzmann constant (1.38×10^{-23} $J \cdot K^{-1}$), and T is the absolute temperature (K).

The photoelectrochemical impedance spectroscopy (PEIS) data were acquired with a perturbation amplitude of 5 mV over a frequency range of 0.1 Hz to 100,000 Hz. From the PEIS measurements conducted under one-sun illumination and the data fitted using equivalent circuit simulations, parameters related to surface states and the surface charge transfer efficiency were determined. The charge transfer efficiency corresponding to the surface states is given by equation

(5):[2]

$$\eta_{\text{surface, PEIS}} = \frac{R_{\text{trapping}}}{R_{\text{trapping}} + R_{\text{ct, trap}}} \#(5)$$

where $R_{\text{ct, trap}}$ and R_{trapping} are the resistances associated with charge trapping at surface states and transfer process from surface states, respectively.

The intensity-modulated photocurrent spectroscopy (IMPS) data were acquired using sinusoidal irradiation at 405 nm over a frequency range from 0.01 Hz to 100 kHz and a potential range from 0.4 to 0.6 V vs. RHE. The maximum imaginary frequency (f_{max}) and the charge transfer efficiency ($\eta_{\text{surface, IMPS}}$) were determined using equation (6) and equation (7):[3, 4]

$$2\pi f_{\text{max}} = k_{\text{rec}} + k_{\text{tran}} \#(6)$$

$$\eta_{\text{surface, IMPS}} = \frac{\text{LFI}}{\text{HFI}} = \frac{k_{\text{tran}}}{k_{\text{rec}} + k_{\text{tran}}} \#(7)$$

where LFI and HFI are the low frequency intersection and high frequency intersection with the real axis.

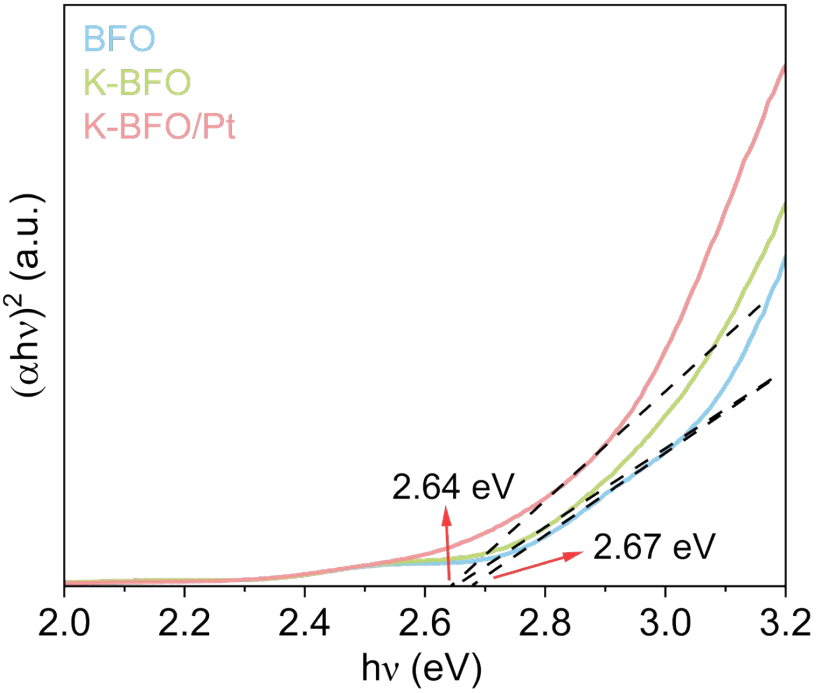

Fig. S1 Tauc plots for band gap fitting of BFO, K-BFO and K-BFO/Pt.

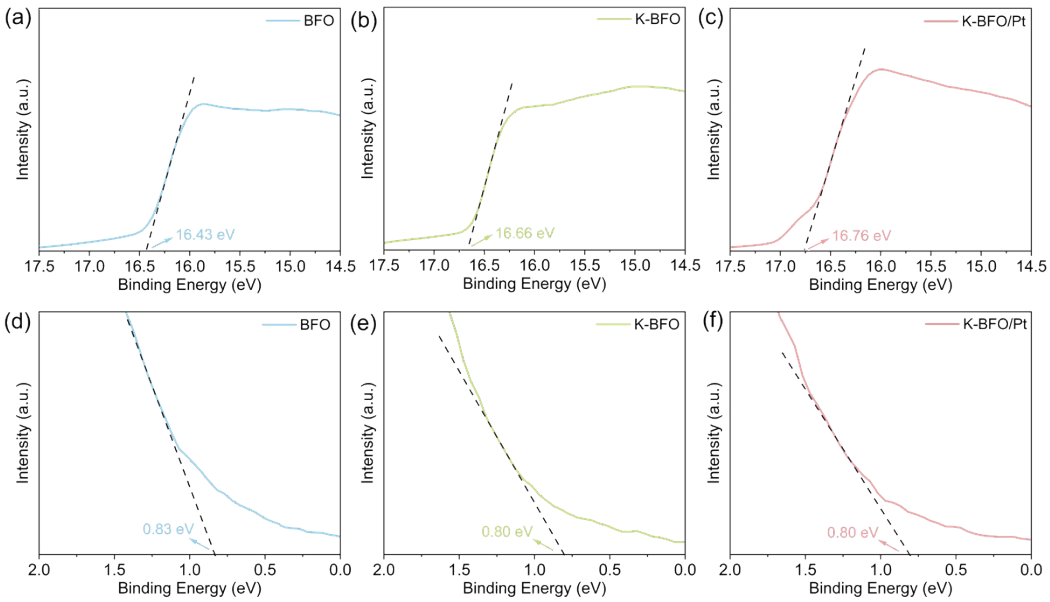

Fig. S2 UPS secondary electron cutoff edge spectra of (a) BFO, (b) K-BFO and (c) K-BFO/Pt. UPS valence band spectrum of (d) BFO, (e) K-BFO and (f) K-BFO/Pt.

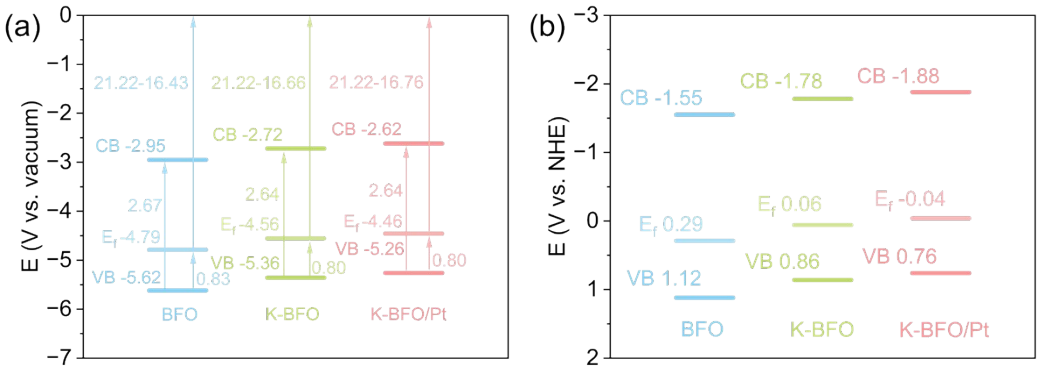

Fig. S3 Energy band structure diagrams of BFO, K-BFO and K-BFO/Pt relative to (a) the vacuum level and (b) the Normal Hydrogen Electrode.

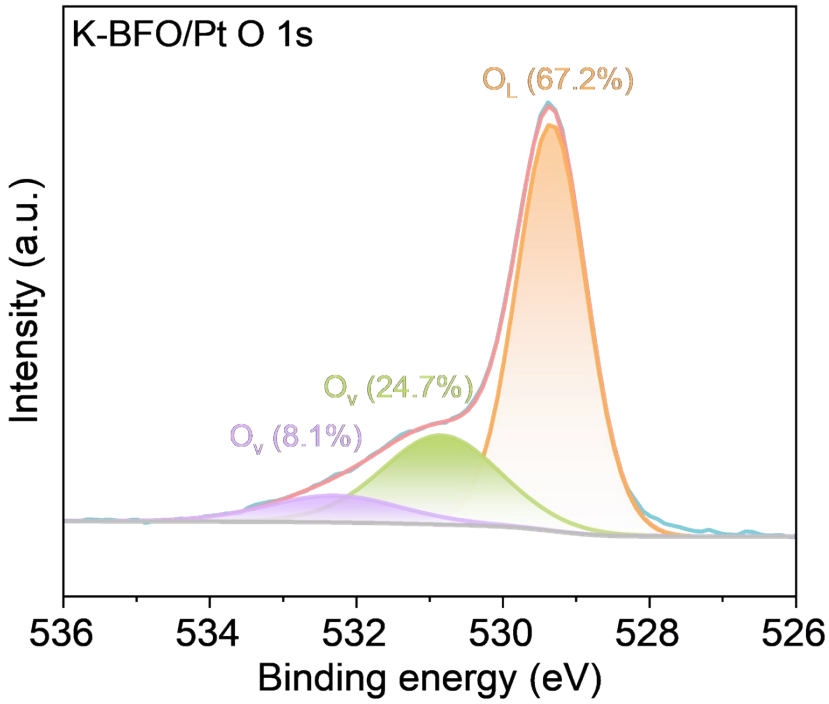

Fig. S4 XPS spectra of O 1s from K-BFO/Pt.

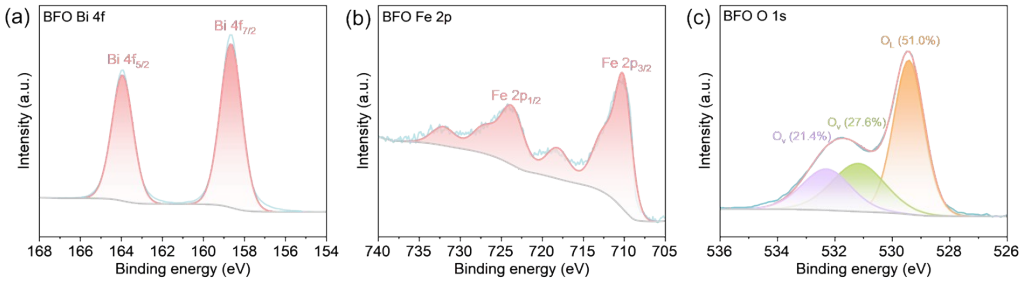

Fig. S5 XPS spectra of (a) Bi 4f, (b) Fe 2p and (c) O 1s from BFO.

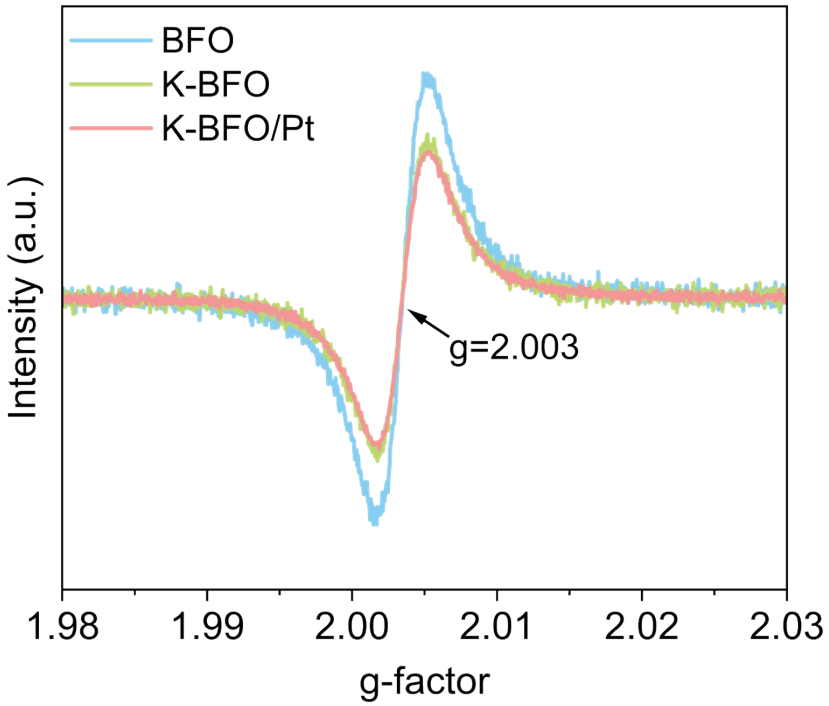

Fig. S6 EPR spectra for BFO, K-BFO and K-BFO/Pt.□

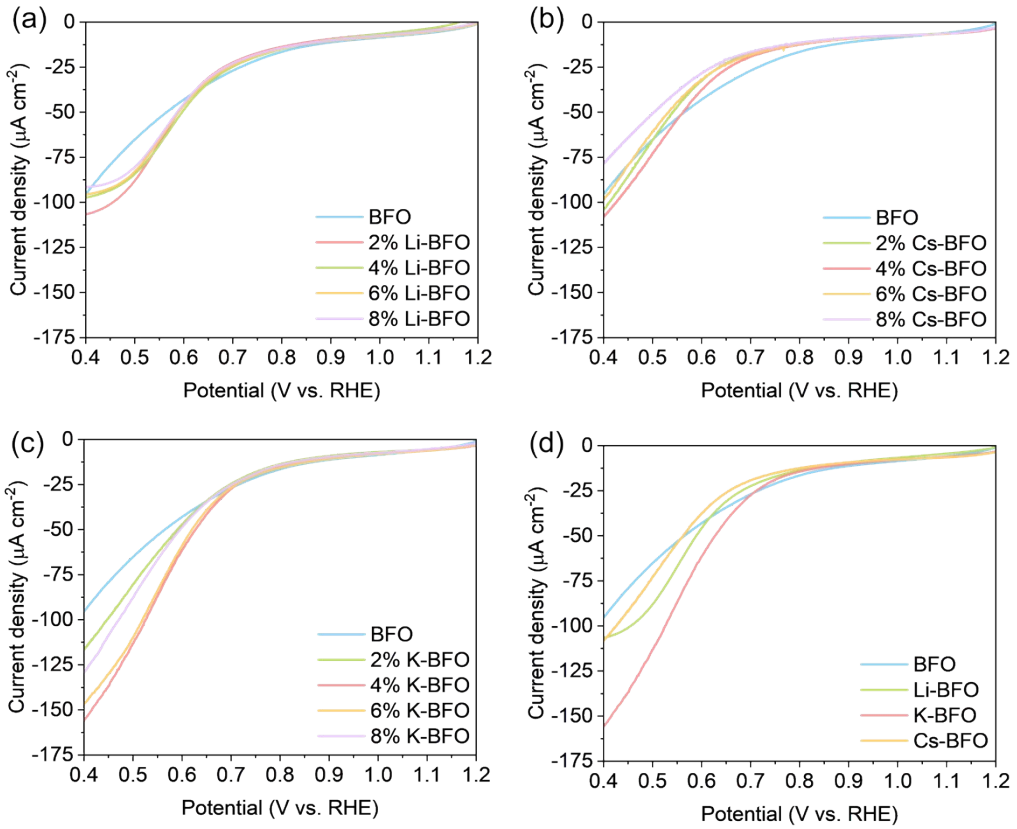

Fig. S7 LSV curves of (a) Li^+-doped samples with gradient doping ratios, (b) Cs^+-doped samples with gradient doping ratios, (c) K^+-doped samples with gradient doping ratios. (d) LSV comparison of optimal samples from each doping system.

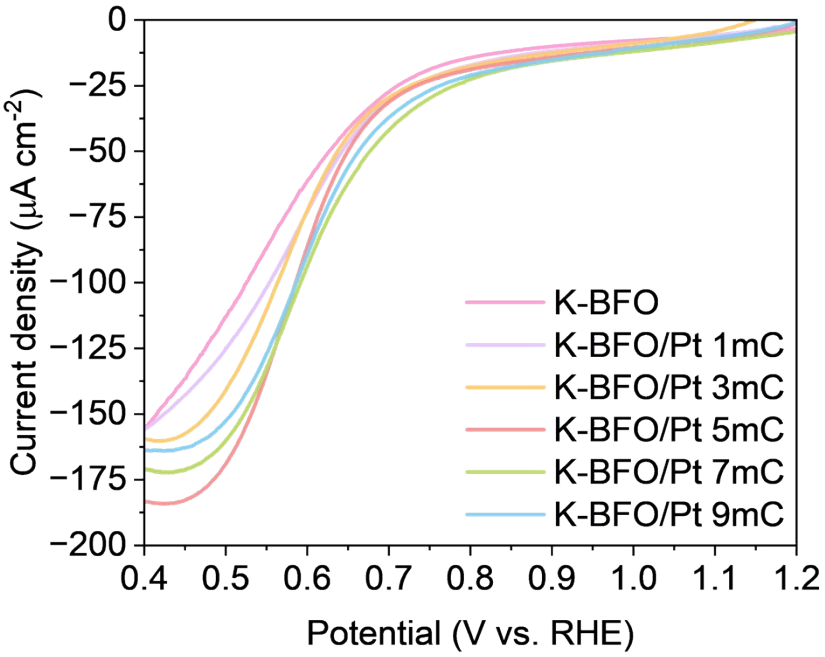

Fig. S8 LSV curves of K-BFO/Pt photoelectrodes with different Pt loadings.

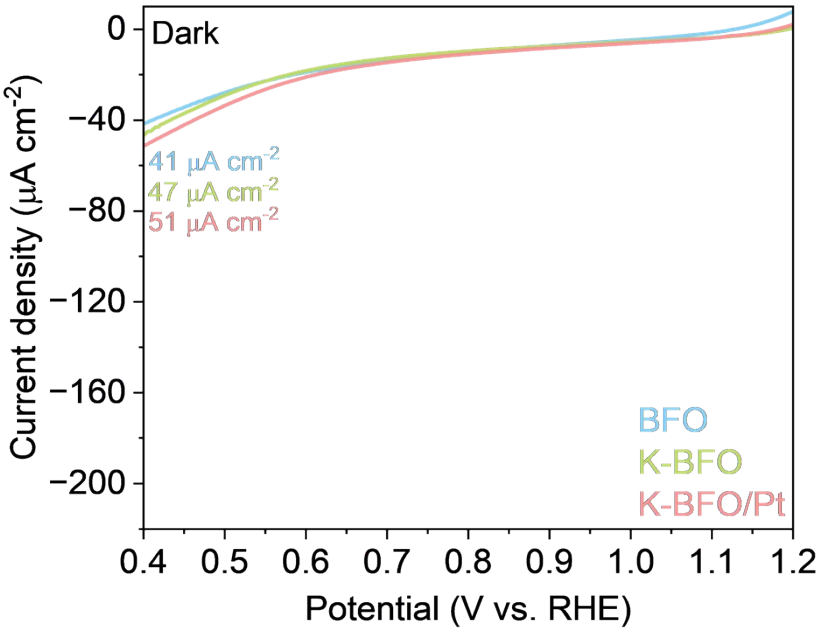

Fig. S9 LSV curves of BFO, K-BFO and K-BFO/Pt under dark.

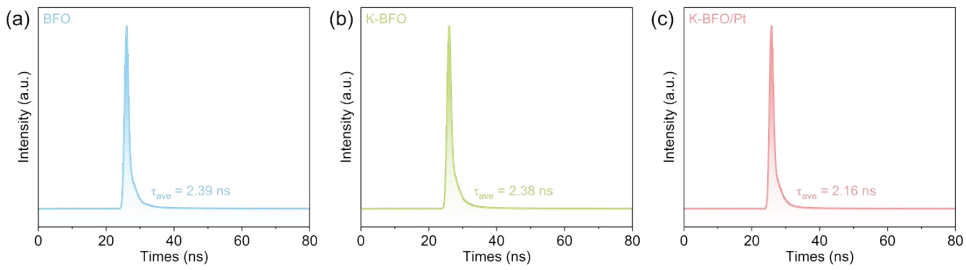

Fig. S10 TRPL decay curves and fitted average carrier lifetime results of (a) BFO, (b) K-BFO and (c) K-BFO/Pt.

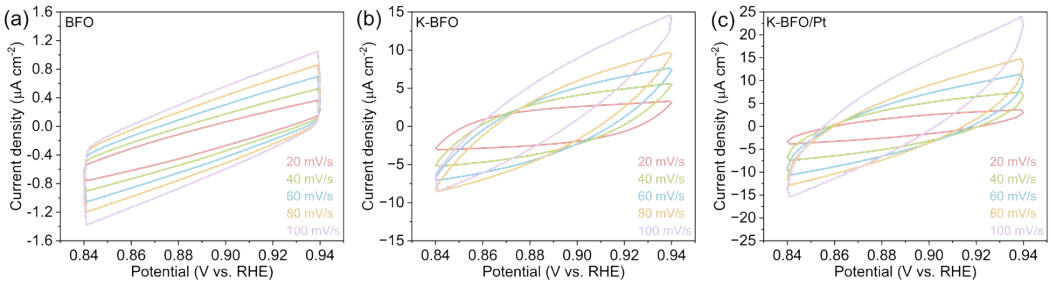

Fig. S11 (a) CV curves of BFO, (b) K-BFO and (c) K-BFO/Pt at different scan rates.

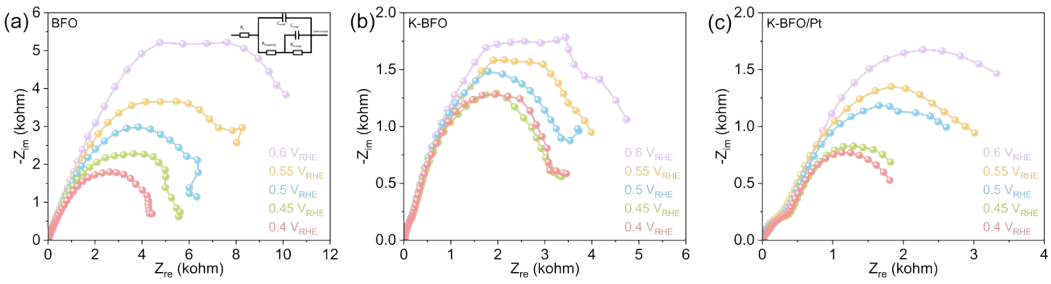

Fig. S12 (a) PEIS Nyquist plots of BFO, (b) K-BFO and (c) K-BFO/Pt under illumination at 0.4 to 0.6 V vs. RHE.

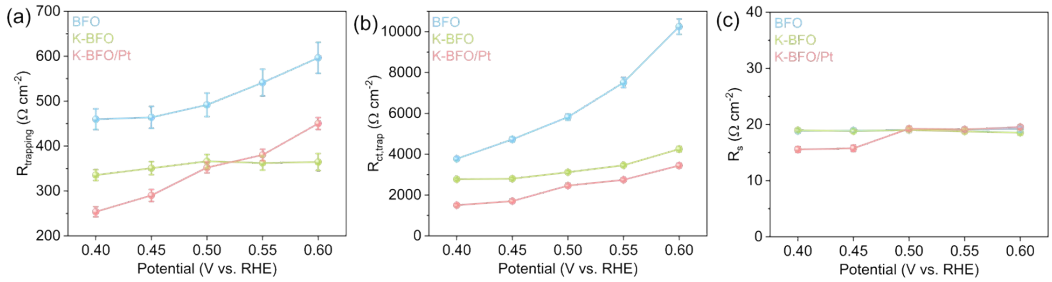

Fig. S13 The resistance values obtained through PEIS fitting and calculation are (a) R_{trapping}, (b) $R_{\text{ct, trap}}$, (c) R_{s}. Error bars stem from the goodness of data fittings.

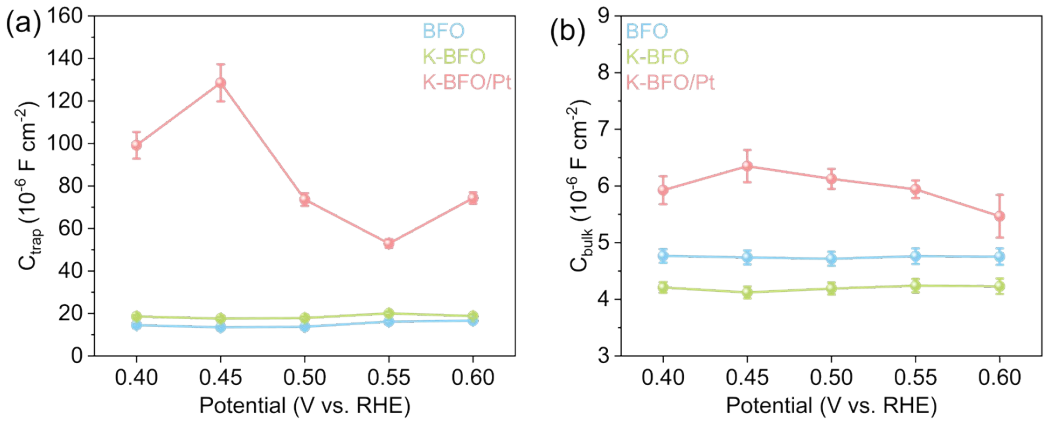

Fig. S14 The capacitance values obtained through PEIS fitting and calculation are (a) C_{trap} and (b) C_{bulk}. Error bars stem from the goodness of data fittings.

References

1. S. Wang, P. Chen, J.-H. Yun, Y. Hu and L. Wang, *Angewandte Chemie International Edition*, 2017, **56** (29), 8500-8504.
2. P. Tang, H. Xie, C. Ros, L. Han, M. Biset-Peiró, Y. He, W. Kramer, A. P. Rodríguez, E. Saucedo, J. R. Galán-Mascarós, T. Andreu, J. R. Morante and J. Arbiol, *Energy & Environmental Science*, 2017, **10** (10), 2124-2136.
3. G.-P. Yi, H. Liu, Y.-P. Zhao, T. H. Tao, Q. Wang and P.-Y. Tang, *Nano Energy*, 2025, **140**, 111066.
4. S. Ren, R.-T. Gao, N. T. Nguyen and L. Wang, *Angewandte Chemie*, 2024, **136** (11), e202317414.